Inorg. Chem. **2007**, *46*, 10587–10593

An Effective Hydrothermal Route for the Synthesis of Multiple PDDA-Protected Noble-Metal Nanostructures

Hongjun Chen, Yuling Wang, and Shaojun Dong*

State Key Laboratory of Electroanalytical Chemistry, Changchun Institute of Applied Chemistry and Graduate School of the Chinese Academy of Sciences, Chinese Academy of Sciences, Changchun, Jilin 130022, People's Republic of China

Received May 17, 2007

In this Article, we demonstrate an effective hydrothermal route for the synthesis of multiple PDDA-protected (PDDA = poly(diallyl dimethylammonium) chloride) noble-metal (including silver, platinum, palladium, and gold) nanostructures in the absence of any seeds and surfactants, in which PDDA, an ordinary and water-soluble polyelectrolyte, acts as both a reducing and a stabilizing agent. Under optimal experimental conditions, Ag nanocubes, Pt and Pd nanopolyhedrons, and Au nanoplates can be obtained, which were characterized by transmission electron microscopy , scanning electron microscopy, energy-dispersive spectroscopy, and X-ray diffraction. More importantly, the nanostructures synthesized show potential applications in surface-enhanced Raman scattering and electrocatalysis, in which Ag nanocubes and Pt nanopolyhedrons were chosen as the examples, respectively.

Introduction

Metal nanoparticles, especially noble metals, are of widely interest due to not only their large surface areas but also their specific functions and potential applications, which are different from those of bulk metal solids.[1] The intrinsic properties of noble-metal nanoparticles are mainly determined by their size, shape, composition, and crystallinity.[2] As a result, the synthesis of size- and shape-controlled noble-metal nanoparticles has attracted worldwide attention in recent years. Currently, various synthetic methods are available for the production of nanoparticles with well-controlled sizes and shapes.[2,3] However, the most convenient and popular method is based on a hydrothermal route, and many noble-metal nanoparticles in the form of spheres,[4] cubes,[5] rods,[6] plates,[7] and wires[8] have been successfully synthesized by the use of this method. These noble-metal nanoparticles can be used as excellent substrates for surface-enhanced Raman scattering (SERS) by adjusting the shape and aspect ratio of the nanoparticles, and the surface plasmon resonance (SPR) can also be tuned to resonate with a laser and optimize the electromagnetic enhancement.[9] In catalysis, it is well-known that both the reactivity and selectivity of Pt nanoparticles in a catalytic reaction are strongly dependent on the crystallographic planes exposed on the surfaces of the nanoparticles.[10]

Polyelectrolytes are often used to modify solid surfaces and colloids, exploiting the electrostatic attraction for their deposition.[11] As a branch of charged polymers, polyelectrolytes can be deposited on solid surfaces layer-by-layer, enabling the control of the total polymer thickness by the

* To whom correspondence should be addressed. E-mail: dongsj@ciac.jl.cn. Fax: +86-431-85689711.

(1) Feldheim, D. L.; Foss, C. A. *Metal Nanoparticles; Synthesis, Characterization, and Applications*; Marcel Dekker: New York, 2002.
(2) (a) Sun, Y.; Xia, Y. *Science* **2002**, *298*, 2176. (b) Sun, Y.; Mayers, B.; Xia, Y. *Nano Lett.* **2003**, *3*, 675. (c) Millstone, J. E.; Park, S.; Shuford, K. L.; Qin, L.; Schatz, G. C.; Mirkin, C. A. *J. Am. Chem. Soc.* **2005**, *127*, 5312.
(3) (a) Yu, Y. Y.; Chang, S. S.; Lee, C. L.; Wang, C. R. C. *J. Phys. Chem. B* **1997**, *101*, 6661. (b) Li, Z.; Liu, Z.; Zhang, J.; Han, B.; Du, J.; Gao, Y.; Jiang, T. *J. Phys. Chem. B* **2005**, *109*, 14445. (c) Pastoriza-Santos, I.; Liz-Marzan, L. M. *Nano Lett.* **2002**, *2*, 903. (d) Li, C.; Cai, W.; Li, Y.; Hu, J.; Liu, P. *J. Phys. Chem. B* **2006**, *110*, 1546.
(4) Wang, X.; Zhuang, J.; Peng, Q.; Li, Y. *Nature* **2005**, *437*, 121.
(5) (a) Yu, D.; Yam, V. W. W. *J. Am. Chem. Soc.* **2004**, *126*, 13200. (b) Lee, H.; Habas, S. E.; Kweskin, S.; Butcher, D.; Somorjai, G. A.; Yang, P. *Angew. Chem., Int. Ed.* **2006**, *45*, 7824.
(6) Hu, J.; Chen, Q.; Xie, Z.; Han, G.; Wang, R.; Ren, B.; Zhang, Y.; Yang, Z.; Tian, Z. *Adv. Funct. Mater.* **2004**, *14*, 183.
(7) (a) Sun, X.; Dong, S.; Wang, E. *Langmuir* **2005**, *21*, 4710. (b) Ah, C. S.; Yun, Y. J.; Park, H. J.; Kim, W. J.; Ha, D. H.; Yun, W. S. *Chem. Mater.* **2005**, *17*, 5558.
(8) Wang, Z.; Liu, J.; Chen, X.; Wan, J.; Qian, Y. *Chem. Eur. J.* **2005**, *11*, 160.
(9) Murphy, C.; Sau, T.; Gole, A.; Orendorff, C. *MRS Bulletin* **2005**, *30*, 349.
(10) (a) Narayanan, R.; El-Sayed, M. A. *J. Am. Chem. Soc.* **2004**, *126*, 7194. (b) Tian, N.; Zhou, Z.; Sun, S.; Ding, Y.; Wang, Z. *Science* **2007**, *316*, 732.
(11) (a) Decher, G. *Science* **1997**, *277*, 1232. (b) Hammond, P. T. *Curr. Opin. Colloid Interface Sci.* **2000**, *4*, 430.

10.1021/ic7009572 CCC: $37.00
Published on Web 11/14/2007

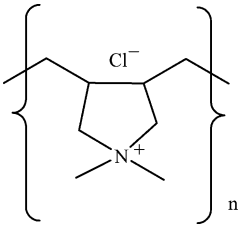

Figure 1. Molecular structure of PDDA; the value of *n* is about 31.

number of layers deposited.[12] Due to electrostatic stabilization, polyelectrolytes can also be used as stabilizing agents for colloids.[13] Recently, it was found that some polyelectrolytes such as poly(sodium acrylate),[14] linear polyethylenimine,[7a,15] and poly(diallyl dimethylammonium) chloride (PDDA)[16] can act as both a reducing and a stabilizing agent in the synthesis of gold nanoparticles. In this Article, we reported an effective hydrothermal route for the synthesis of polyelectrolyte-protected noble-metal nanostructures by use of PDDA (the molecular structure is shown in Figure 1), which acts as both a reducing and a stabilizing agent. As an extension of our previously reported paper about the synthesis of PDDA-protected gold sphere nanoparticles,[16] this Article is intended to make this synthetic route more effective for the synthesis of multiple PDDA-protected noble-metal (including silver, platinum, palladium, and gold) nanostructures in the absence of any seeds and surfactants. Whereas the Ag nanocubes obtained show potential application in SERS, which can be used as a SERS substrate with high sensitivity for the probe molecule of *p*-aminothiophenol (*p*-ATP), the Pt nanopolyhedrons show good electrocatalytic ability for O_2 reduction.

Experimental Section

Chemicals. PDDA (50 wt % in water, $M_n \sim 5000$, M_w 20 000) and *p*-ATP were purchased from Aldrich. $AgNO_3$, H_2PtCl_6, $PdCl_2$, HCl, and $NH_3 \cdot H_2O$ (25%) were obtained from the Beijing Chem. Co. All reagents were used as received without further purification. The water used was purified through a Millipore system.

Synthesis. In typical experiments, 800 μL of PDDA (0.27 M, the concentration was calculated in terms of the repeating unit), 10 mL of $AgNO_3$ (20 mM) and 400 μL of $NH_3 \cdot H_2O$ (25%, $NH_3 \cdot H_2O$ was added to get rid of the AgCl produced); 200 μL of PDDA (0.27 M), 5 mL of water, and 600 μL of H_2PtCl_6 (19.3 mM); 1200 μL of PDDA (0.27 M), 5 mL of water, and 600 μL of H_2PdCl_4 (56.4 mM, 1 g of $PdCl_2$ was dissolved in 36 mL of 0.2 M aqueous HCl solution and then diluted to a 100 mL volume with water); and 600 μL of PDDA (0.27 M), 5 mL of water, and 600 μL of $HAuCl_4$ (24.3 mM) were mixed under vigorous stirring for 0.5 h. Then the different mixtures were transferred into 15 mL Teflon-sealed autoclaves and heated at 170 °C for 16 h, 140 °C for 40 h, 190 °C for 40 h, and 170 °C for 12 h, respectively. After the reaction, the autoclaves were allowed to cool in air and the suspensions were centrifuged for 20 min at 8000, 12000, and 8000 rpm for Ag, Pt, and Pd, respectively, and the precipitates were washed with purified water and centrifuged/rinsed three times; for Au, the product precipitated naturally without centrifugation due to its very high specific gravity.

Instrumentation. The samples for transmission electron microscopy (TEM), X-ray diffraction (XRD), scanning electron microscopy (SEM), energy-dispersive spectroscopy (EDS), and X-ray photoelectron spectra (XPS) characterization were prepared by placing a drop of colloidal solution on a carbon-coated copper grid, clean glass, indium tin oxide (ITO), or silicon plates, respectively. TEM measurement was made on a JEOL 2000 transmission electron microscope operated at an accelerating voltage of 200 kV. The XRD pattern was collected on a D/Max 2500 V/PC X-ray diffractometer using Cu (40 kV, 200 mA) radiation. The SEM and EDS data were obtained on a XL30 ESEM FEG scanning electron microscope equipped with X-ray EDS capability at an accelerating voltage of 20 kV. The XPS analysis was performed on an ESCLAB MKII instrument using Mg as the exciting source. The charging calibration was performed by referring the C1s to the binding energy at 284.6 eV. The operating pressure in the analysis chamber was below 10^{-9} Torr with a analyzer pass energy of 50 eV. Fourier transform infrared (FTIR) analysis was carried out using a Nicolet 520 SXFTIR spectrometer. The spectra were obtained by mixing the sample with KBr, acquiring an average of 120 scans and 4 cm^{-1} resolution. SERS spectra were recorded with a J-Y T64000 microRaman spectrometer (Jobin-Yvon, France) equipped with a liquid nitrogen-cooled CCD detector. The spectra were obtained by using the 514.5 nm line of a continuous-wave Ar^+ ion laser (SpectraPhysics 2713), the accumulation time was 10 s, and the incident power was 10 mW. Cyclic voltammetry was performed with a CHI 600 electrochemical workstation (CH Instrument Co., U.S.) in a conventional three-electrode electrochemical cell with the Pt nanopolyhedrons-modified ITO as the working electrode, a large platinum foil as the auxiliary electrode, and KCl-saturated Ag/AgCl as the reference electrode. The Pt nanopolyhedrons-modified ITO electrode was prepared by placing a drop of colloidal solution on an ITO surface and dried under an infrared lamp. The real surface areas of bulk Pt electrode and Pt nanopolyhedrons-modified ITO electrode were estimated by graphical integration of the area under the hydrogen-adsorption peak according to a well-established method[17] (assuming a monolayer of H adatoms requires 210 $\mu C \cdot cm^{-2}$). The current density is used as the ratio of current to the real surface area. For the blank ITO electrode, the current density is the value based on its geometric surface area.

Results and Discussion

Synthesis and Characterization of the Multiple PDDA-Protected Noble-Metal Nanostructures. As shown in Figure 2, multiple noble-metal nanostructures including Ag nanocubes, Pt and Pd nanopolyhedrons, and Au nanoplates are obtained by using the hydrothermal route. The inset in Figure 2a shows a typical TEM image of Ag nanocubes, showing that these Ag nanocubes are single crystals with sharp corners and edges with about 58 nm in average edge length. Pt and Pd nanopolyhedrons have average sizes of 10 and 60 nm (Figures 2b and 2c), respectively. While the Au nanoplates with different sizes (from 10 to 200 μm) are mainly in the triangle, truncated triangle, and hexagon shapes (Figure 2d), the thickness of the Au nanoplates is about 311

(12) Shiratori, S. S.; Rubner, M. F. *Macromolecules* **2000**, *33*, 4213.
(13) (a) Elechiguerra, J. L.; Reyes-Gasgab, J.; Yacaman, M. J. *J. Mater. Chem.* **2006**, *16*, 3906. (b) Pugh, T. L.; Heller, W. *J Polym. Sci.* **1960**, *47*, 219.
(14) Hussain, I.; Brust, M.; Papworth, A. J.; Cooper, A. I. *Langmuir* **2003**, *19*, 4831.
(15) Sun, X.; Dong, S.; Wang, E. *Polymer* **2004**, *45*, 2181.
(16) Chen, H.; Wang, Y.; Wang, Y.; Dong, S.; Wang, E. *Polymer* **2006**, *47*, 763.
(17) Trasatti, S.; Petrii, O. A. *J. Electroanal. Chem.* **1992**, *327*, 353.

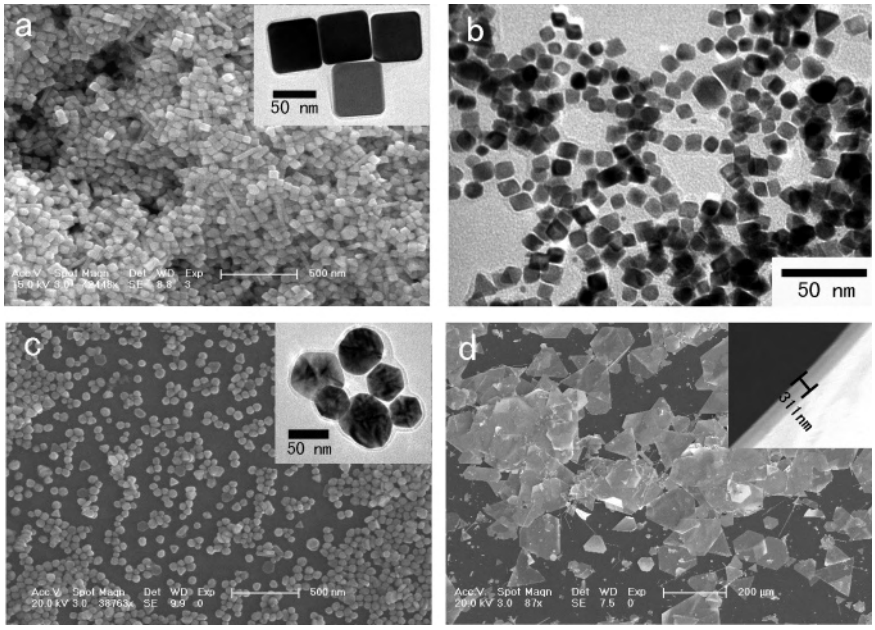

Figure 2. Typical SEM and TEM images of the PDDA-protected Ag nanocubes (a), Pt nanopolyhedrons (b), Pd nanopolyhedrons (c), and Au nanoplates (d).

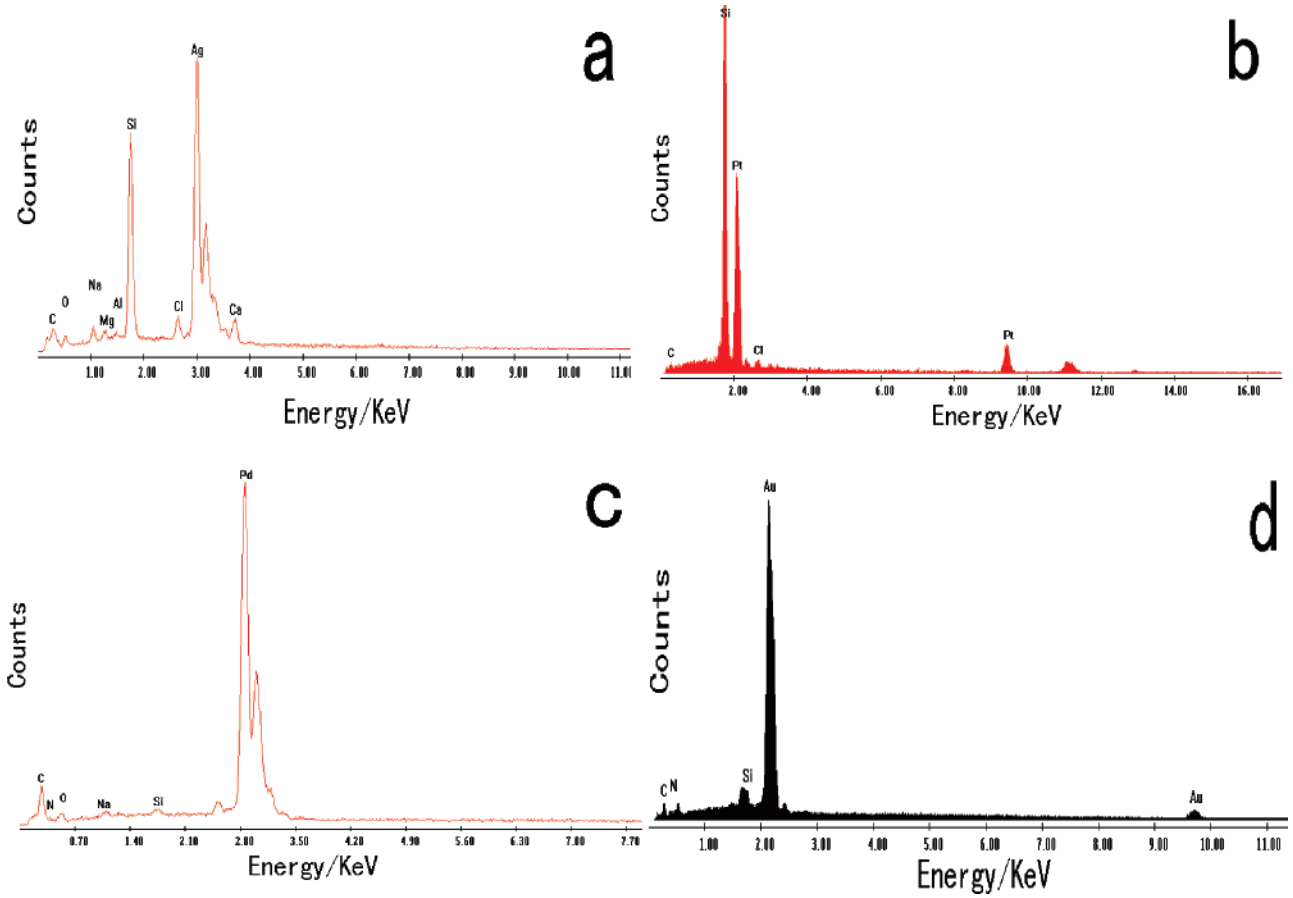

Figure 3. Typical EDS results of the PDDA-protected Ag nanocubes (a), Pt nanopolyhedrons (b), Pd nanopolyhedrons (c), and Au nanoplates (d).

nm as shown in the inset in Figure 2d. EDS spectra clearly show the corresponding peaks of Ag, Pt, Pd, and Au (Figure 3), demonstrating that the main components of these four nanostructures are metallic Ag, Pt, Pd, and Au, respectively. Figure 4 gives four representative XRD patterns of these four noble-metal nanostructures, and the peaks can be indexed to the face-centered cubic (fcc) Ag, Pt, Pd, and Au structures, respectively. After calculation, the lattice constants are 4.074, 3.939, 3.916, and 4.098 Å for Ag nanocubes, Pt and Pd nanopolyhedrons, and Au nanoplates, respectively, which are values in good agreement with their standard file (in JCPDS card, a = 4.071, 3.938, 3.908, and 4.078 Å for Ag, Pt, Pd,

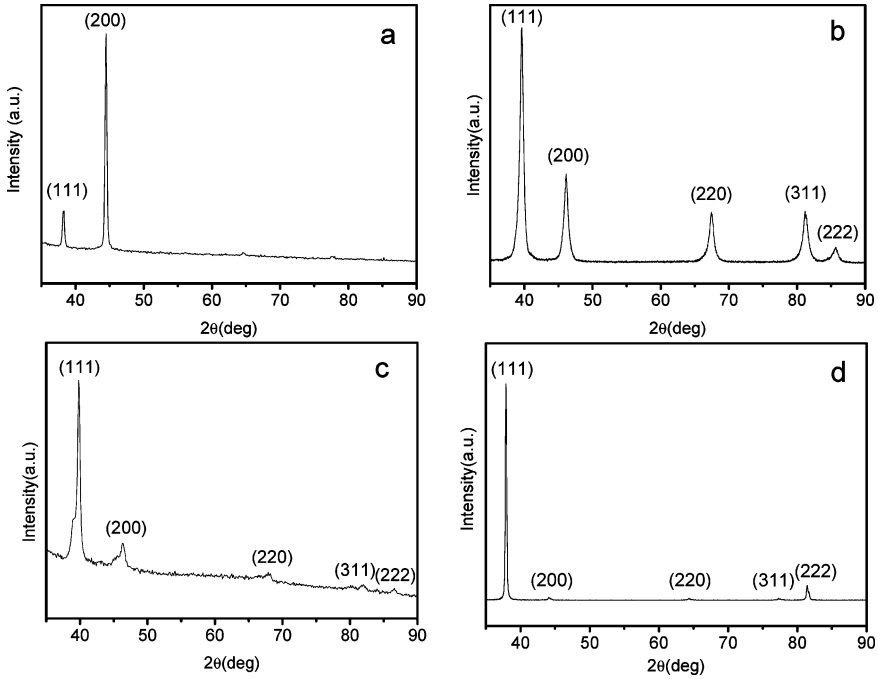

Figure 4. Typical XRD patterns of the PDDA-protected Ag nanocubes (a), Pt nanopolyhedrons (b), Pd nanopolyhedrons (c), and Au nanoplates (d).

Table 1. Summary of the SEM, TEM, XRD, and EDS Data

	SEM and TEM		XRD				EDS
	main shape	average size (nm)	lattice constant (Å)		intensity ratio of (111)/(200)		main peaks
Ag	nanocubes	about 58	4.074	4.071[a]	0.167	2.22[a]	Ag, C
Pt	nanopolyhedrons	about 10	3.939	3.938[b]	2.845	2.2[b]	Pt, C, Cl
Pd	nanopolyhedrons	about 60	3.916	3.908[c]	8.2	2.26[c]	Pd, C, N
Au	nanoplates	10×10^3 to 200×10^3, about 311 in thickness	4.098	4.078[d]	92.4	1.92[d]	Au, C, N

[a] Refer to JCPDS card 87-0719. [b] Refer to JCPDS card 87-0642. [c] Refer to JCPDS card 87-0643. [d] Refer to JCPDS card 04-0784.

and Au, respectively). By comparing the intensity ratio of (111) to (200) with its corresponded conventional value, it is found that the value for Ag nanocubes is much lower than the conventional value (0.167 versus 2.22), indicating that these Ag nanocubes are preferentially oriented with their {100} planes parallel to the supporting substrate.[5a,18] The values for Pt and Pd nanopolyhedrons and gold nanoplates are higher than their corresponding conventional values (for Pt, 2.845 versus 2.2; for Pd, 8.2 versus 2.26; for Au, 92.4 versus 1.92), demonstrating that the faces of these nanostructures are dominated by {111} planes at different degrees.[19−21] To clarify these comparisons, we also summarize these data in Table 1.

As a representative case, we chose synthesized Pd polyhedrons to examine the molar ratio between PDDA and H_2PdCl_4's influence on the morphologies of the Pd products thus formed. Two samples were prepared under conditions identical to those of the Pd nanopolyhedrons shown in Figure 2c, but the the volume of PDDA used (0.27 M) was decreased from 1200 μL to 600 and 200 μL, respectively. When the volume of PDDA (0.27 M) was reduced to 600 μL, the size of the Pd polyhedrons was not uniform; many of them are about 200 nm in edge length, and some large Pd polyhedrons can be clearly seen (Figure 5a). By continuously decreasing the volume of PDDA used (0.27 M) to 200 μL, many large Pd polyhedrons (about 1−2 μm in size) can be obtained, as shown in Figure 5b. Therefore, the molar ratio of PDDA to H_2PdCl_4 is the key factor that determines the size of Pd polyhedrons.

To clearly characterize the structure change of PDDA after reaction, FTIR and XPS measurements are adopted, as shown parts a and b of Figure 6, respectively. The FTIR spectrum of PDDA-protected Au nanoplates (curve b) is similar to that of the original PDDA (curve a), although a slight shift of wavenumber is observed. The most difference between these two FTIR spectra in Figure 6a is the appearance of two new peaks at 1385 and 831 cm^{-1} in curve b, which are assigned to N═O and C−N vibrations, respectively.[22] This may prove that the nitroso group is produced after PDDA reacted with $HAuCl_4$. Figure 6b gives the typical XPS spectra of the N 1s electron region of PDDA (curve a) and PDDA-

(18) Im, S. H.; Lee, Y. T.; Wiley, B.; Xia, Y. *Angew. Chem., Int. Ed.* **2005**, *44*, 2154.
(19) Chen, J.; Herricks, T.; Geissler, M.; Xia, Y. *J. Am. Chem. Soc.* **2004**, *126*, 10854.
(20) Xiong, Y.; McLellan, J. M.; Chen, J.; Yin, Y.; Li, Z. Y.; Xia, Y. *J. Am. Chem. Soc.* **2005**, *127*, 17118.
(21) Sun, X.; Dong, S.; Wang, E. *Angew. Chem., Int. Ed.* **2004**, *43*, 6360.
(22) Socrates, G. *Infrared and Raman Characteristic Group Frequencies Tables and Charts*, 3rd ed.; John Wiley & Sons, Ltd.: Chichester, U.K., 2001.

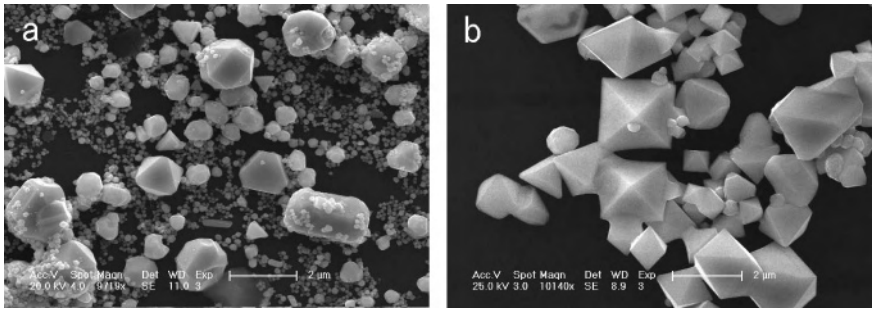

Figure 5. Typical SEM images of the PDDA-protected Pd polyhedrons synthesized under conditions identical to those shown in Figure 2c, but with the volume of PDDA (0.27 M) reduced from 1200 μL to 600 (a) and 200 (b) μL, respectively.

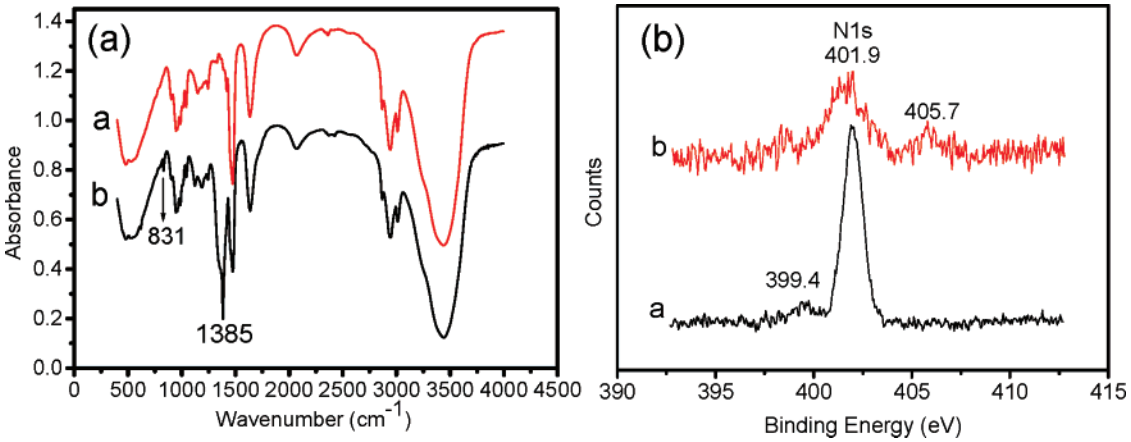

Figure 6. (a) FTIR spectra of PDDA (curve a) and PDDA-protected Au nanoplates (curve b). (b) XPS spectra of N 1s electron region of PDDA (curve a) and PDDA-protected Au nanoplates (curve b).

protected Au nanoplates (curve b). Comparing the N 1s spectrum of PDDA to that of PDDA-protected Au nanoplates, the principal peak at 401.9 eV, due to N^+, is preserved; a second peak, at 399.4 eV, due to an uncharged component in PDDA almost disappears,[23] while a new peak appears at 405.7 eV, possibly due to the presence of the nitroso group in the PDDA-protected Au nanoplates, indicating part of the N or N^+ in PDDA has been oxidized to the nitroso group,[24] which is agrees well with the aforementioned FTIR data.

On the basis of the above analysis, the reduction of noble-metal salts by the polyelectrolyte PDDA can be applied as an effective hydrothermal route for the synthesis of multiple noble-metal nanostructures including Ag, Pt, Pd, and Au. The major advantage of this synthetic route is that the polyelectrolyte PDDA can work as both a reducing and a stabilizing agent. From the synthetic conditions, it can also be determined that PDDA is a mild reductant. Perhaps just about this point, PDDA can reduce noble-metal salts at a sufficiently slow rate so that the growth becomes kinetically controlled, particularly in the nucleation stage, leading to the formation of highly anisotropic nanostructures with certain preferential growth directions.[25] It is also well-known that the surface energies associated with different crystallographic planes are usually different, and a general sequence of $\gamma_{\{111\}} < \gamma_{\{100\}} < \gamma_{\{110\}}$ may hold. Therefore, it is commonly accepted that the shape of an fcc nanocrystal is mainly determined by the ratio (R) of the growth rate along the [100] direction versus that of the [111] direction.[26] In this system, due to the fact that the {111} facet of the fcc noble metals (including Pt, Pd, and Au) has the lowest surface energy and PDDA probably preferentially adsorbs on the sites of the {111} facet, the noble metal's nuclei obviously slows (or prevents) the growth on the {111} facet and promotes a highly anisotropic crystal growth such as that along the [100] and/or [110] direction/s. Thus, {111}-faceted Pt and Pd nanopolyhedrons and gold nanoplates are

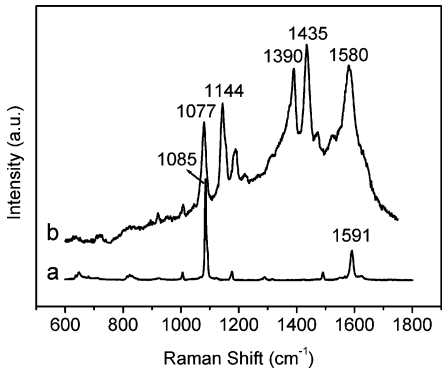

Figure 7. SERS spectrum of 10^{-7} M *p*-ATP on the PDDA-protected Ag nanocubes (curve b) and normal Raman spectrum of solid *p*-ATP (curve a).

(23) Yang, D. Q.; Rochette, J. F.; Sacher, E. *J. Phys. Chem. B* **2005**, *109*, 4481.
(24) Price, B. K.; Hudson, J. L.; Tour, J. M. *J. Am. Chem. Soc.* **2005**, *127*, 14867.
(25) Xiong, Y.; Washio, I.; Chen, J.; Cai, H.; Li, Z.; Xia, Y. *Langmuir* **2006**, *22*, 8563.
(26) Wang, Z. L. *J. Phys. Chem. B* **2000**, *104*, 1153.

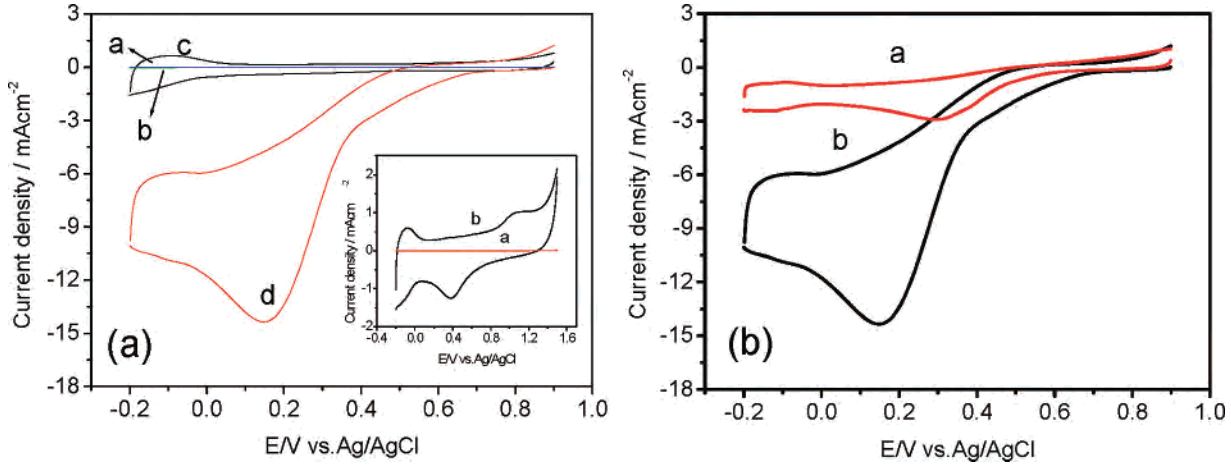

Figure 8. (a) CVs of O_2 reduction at the bare (curve a and b) and Pt nanopolyhedrons-modified ITO electrodes (curves c and d) in N_2-saturated (curves a and c) and air-saturated (curves b and d) 0.1 M H_2SO_4. Inset: CVs of bare (curve a) and Pt nanopolyhedrons-modified ITO (curve b) electrodes in N_2-saturated 0.1 M H_2SO_4. (b) CVs of O_2 reduction at the bulk Pt electrode (curve a) and Pt nanopolyhedrons-modified ITO electrode (curve b) in air-saturated 0.1 M H_2SO_4. Scan rate, 50 mV·s^{-1}.

formed eventually. For the case of Ag nanocubes, the introduction of a foreign reagent (NH_3·H_2O) plays an important role in greatly changing the relative growth rates along certain directions; that is, the Ag nuclei can significantly reduce the growth rate along the [100] direction and/or enhance the growth rate along the [111] direction, and ultimately, Ag cubic particles result.[5,27]

SERS of *p*-ATP on the PDDA-Protected Ag Nanocubes and Electrocatalytic Property of the PDDA-Protected Pt Nanopolyhedrons. Metal nanoparticles have shown wide applications in optical and catalysis due to their inherent properties such as SPR and high density. We choose PDDA-protected Ag nanocubes and Pt nanopolyhedrons as representative examples for the investigation of SERS and electrocatalytic properties, respectively. Here, *p*-ATP was chosen as a probe molecule because it can form a self-assembled monolayer on a metal surface and most of its prominent Raman bands have been assigned. Figure 7 shows the SERS spectrum of 10^{-7} M *p*-ATP (curve b) on Ag nanocubes and the normal Raman spectrum of solid *p*-ATP (curve a). Comparing the SERS spectrum of *p*-ATP with that of the normal Raman spectrum of solid *p*-ATP, the noticeable differences in the SERS spectra of these Ag nanocubes are those of frequency shift and intensity change for most of the bands, such as the ν_{CS} band shifts from 1085 to 1077 cm^{-1} and the ν_{CC} band shifts from 1591 to 1580 cm^{-1}. These changes of several main bands indicate that the thiol group in *p*-ATP is in direct contact with the Ag nanocubes.[28] It can also be clearly observed that the two main vibration modes a_1 and b_2 all appear in the SERS spectrum of *p*-ATP on Ag nanocubes, in which the peaks at 1580, 1435, 1390, and 1144 cm^{-1} ascribed to the b_2 vibration mode suggest that the enhancement via the charge-transfer resonance mechanism is significant, while the peak at 1077 cm^{-1} belonging to the a_1 vibration mode implies that an electromagnetic mechanism is also important.[29] Therefore, the PDDA-protected Ag nanocubes can be used as SERS substrate with high sensitivity.

Regarding the use of Pt as the most efficient catalyst for O_2 reduction, the PDDA-protected Pt nanopolyhedrons are expected to keep these properties for their future applications as cathodes in fuel cells. The inset in Figure 8a gives the representative cyclic voltammograms (CVs) obtained from −0.2 to 1.5 V at the bare and Pt nanopolyhedrons-modified ITO electrode in N_2-saturated 0.1 M H_2SO_4. It can be seen that CV of Pt nanopolyhedrons-modified ITO electrode (curve b) is similar to that of a polycrystalline Pt electrode, displaying the hydrogen adsorption/desorption peaks and preoxidation/reduction peaks.[30] No current response occurs at the bare ITO electrode (curve a) in this potential region. CVs for O_2 reduction at these two electrodes in air-saturated 0.1 M H_2SO_4 are shown in Figure 8a. Compared with that of the bare ITO (curve b), at the Pt nanostructures-modified ITO electrode a remarkable cathodic peak occurs at 0.19 V (curve d), attributed to the catalytic reduction of O_2. While these two electrodes only give small background current in N_2-saturated 0.1 M H_2SO_4 (curves a and c), the much more positive shift of peak potential and higher increase in the peak current for O_2 reduction indicates that a significant electrocatalytic effect resulted from the Pt nanopolyhedrons. To further demonstrate the high electrocatalytic ability of the Pt nanopolyhedrons, we also use a bulk Pt electrode for comparison, as shown in Figure 8b. It can be seen that the CV for O_2 reduction at the Pt nanopolyhedrons-modified ITO electrode (curve b) shows much higher current density than that of the bulk Pt electrode (curve a). Meanwhile, the overpotential toward O_2 reduction is also increased, demonstrating the stabilizing agent PDDA on the Pt nanopolyhedrons' surface somewhat hampers their electrocatalytic ability toward O_2 reduction.

(27) Kim, F.; Connor, S.; Song, H.; Kuykendall, T.; Yang, P. *Angew. Chem., Int. Ed.* **2004**, *43*, 3673.
(28) (a) Zheng, J.; Li, X.; Gu, R.; Lu, T. *J. Phys. Chem. B* **2002**, *106*, 1019. (b) Wang, Y.; Cheng, H.; Dong, S.; Wang, E. *J. Chem. Phys.* **2006**, *125*, 044710.
(29) Osawa, M.; Matsuda, N.; Yoshii, K.; Uchida, I. *J. Phys. Chem.* **1994**, *98*, 12702.
(30) Huang, M.; Shao, Y.; Sun, X.; Chen, H.; Liu, B.; Dong, S. *Langmuir* **2005**, *21*, 323.

Conclusions

In this Article, we demonstrate an effective hydrothermal route for the synthesis of multiple PDDA-protected noble-metal nanostructures including Ag nanocubes, Pt and Pd nanopolyhedrons, and Au nanoplates in the absence of any seeds and surfactants. The major advantage of this synthetic route is that PDDA, an ordinary and water-soluble polyelectrolyte, can work as both a reducing and a stabilizing agent. As the representative PDDA-protected noble-metal nanostructures, the Ag nanocubes can be used as a SERS substrate with high sensitivity and the Pt nanopolyhedrons show good electrocatalytic ability for O_2 reduction. It is also expected that these PDDA-protected noble-metal nanostructures can find more applications in biosensors, SPR, etc.

Acknowledgment. This work was supported by the National Natural Science Foundation of China (Grant Nos. 20427003, 20575064, and 20675076).

IC7009572